

Petrophysics Vol. 64 No. 3, June 2023

TABLE OF CONTENTS PAGE

ARTICLES

Hybrid Technique for Setting Initial Water Saturation on Core Samples

Victor Fernandes, Benjamin Nicot, Fabrice Pairoys, Henri Bertin, Jean Lachaud, and Cyril Caubit
PETROPHYSICS, VOL. 64, NO. 3 (JUNE 2023); PAGES 325–339; 26 FIGURES, 4 TABLES.
DOI:10.30632/PJV64N3-2023a1

Wireless Acquisition for Resistivity Index in Centrifuge – WiRI: A Comparative Study of Three Pc-RI Methods

Quentin Danielczick, Ata Nepesov, Laurent Rochereau, Sandrine Lescoulie, Victor De Oliveira Fernandes, and Benjamin Nicot
PETROPHYSICS, VOL. 64, NO. 3 (JUNE 2023); PAGES 340–352; 13 FIGURES, 5 TABLES.
DOI:DOI:10.30632/PJV64N3-2023a2

Analytical Models for Predicting the Formation Resistivity Factor and Resistivity Index at Overburden Conditions

Meysam Nourani, Stefano Pruno, Mohammad Ghasemi, Muhamet Meti Fazlija, Byron Gonzalez, and Hans-Erik Rodvelt
PETROPHYSICS, VOL. 64, NO. 3 (JUNE 2023); PAGES 353–366; 13 FIGURES, 5 TABLES.
DOI:10.30632/PJV64N3-2023a3

Advanced Digital-SCAL Measurements of Gas Trapped in Sandstone

Ying Gao, Tibi Sorop, Niels Brussee, Hilbert van der Linde, Ab Coorn, Matthias Appel, and Steffen Berg
PETROPHYSICS, VOL. 64, NO. 3 (JUNE 2023); PAGES 368–383; 16 FIGURES.
DOI:10.30632/PJV64N3-2023a4

Shale Characterization Using T1-T2* Magnetic Resonance Relaxation Correlation Measurement at Low and High Magnetic Fields

Mohammad Sadegh Zamiri, Jiangfeng Guo, Florea Marica, Laura Romero-Zerón, and Bruce J. Balcom
PETROPHYSICS, VOL. 64, NO. 3 (JUNE 2023); PAGES 384–401; 14 FIGURES, 1 TABLE.
DOI:10.30632/PJV64N3-2023a5

Angle-Dependent Ultrasonic Wave Reflection for Estimating High-Resolution Elastic Properties of Complex Rock Samples

Daria Olszowska, Gabriel Gallardo-Giozza, Domenico Crisafulli, and Carlos Torres-Verdín
PETROPHYSICS, VOL. 64, NO. 3 (JUNE 2023); PAGES 402–419; 15 FIGURES, 4 TABLES.
DOI:10.30632/PJV64N3-2023a6

NMR-Mapped Distributions of Dielectric Dispersion

James Funk, Michael Myers, and Lori Hathon
PETROPHYSICS, VOL. 64, NO. 3 (JUNE 2023); PAGES 421–437; 31 FIGURES, 2 TABLES.
DOI:10.30632/PJV64N3-2023a7

THz Imaging to Map the Lateral Microporosity Distribution in Carbonate Rocks

Shannon L. Eichmann, Jacob Bouchard, Hooisweng Ow, Doug Petkie, and Martin E. Poitzsch
PETROPHYSICS, VOL. 64, NO. 3 (JUNE 2023); PAGES 438–447; 5 FIGURES.
DOI:10.30632/PJV64N3-2023a8

Experimental Time-Lapse Visualization of Mud-Filtrate Invasion and Mudcake Deposition Using X-Ray Radiography

Pierre Aéréns, Carlos Torres-Verdín, and Nicolas Espinoza
PETROPHYSICS, VOL. 64, NO. 3 (JUNE 2023); PAGES 448–461; 13 FIGURES, 2 TABLES.
DOI:10.30632/PJV64N3-2023a9

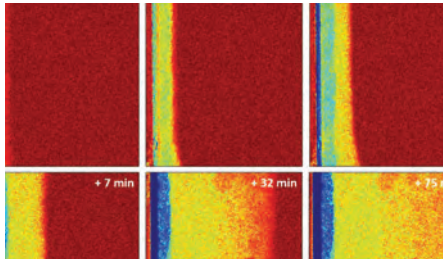
HOW TO ACCESS ARTICLES

SPWLA Members have access to journals through paid membership packages. Annual dues include digital issues of Petrophysics Journal. Sign into your account Visit tab Publications → Petrophysics Papers.

Expired Membership? Sign into your account <https://www.spwla.org/SPWLA/Members/MemberHome.aspx> to make payment. Reset maybe delayed by until the next SPWLA business day.

Become a member? Join now https://www.spwla.org/SPWLA/Membership/Join_Now/Become_a_Member.aspx?hkey=902c4b79-2640-4b86-a56b-609e20248ba6

JUNE 2023 PAPER SUMMARIES



Aérens et al.

PAGES 448–461

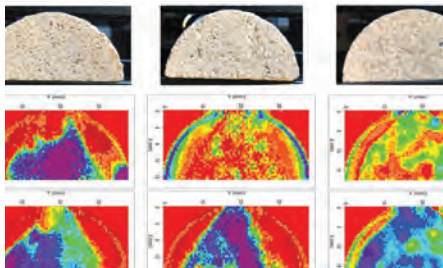
Experimentation is needed to accurately describe and quantify the effects of mud invasion on borehole geophysical measurements. The authors developed a new high-resolution experimental method to investigate these effects using 2D X-ray radiography and thin rectangular samples. The experimental method successfully examines the effects of rock heterogeneity, bedding plane orientation, and anisotropy on the spatial distribution of fluids and mudcake formation resulting from mud-filtrate invasion.



Danielczick et al.

PAGES 340–352

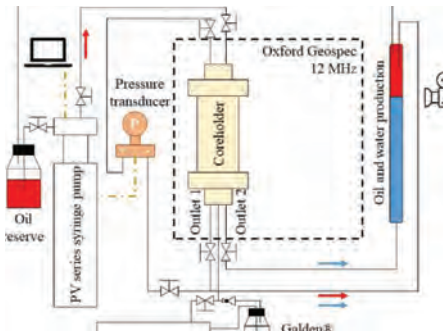
Since 2021, the wireless resistivity index (WiRI) method allows the acquisition of capillary pressure and resistivity index in a matter of days. This paper examines the advantages and drawbacks of this method compared to two others: porous plate and ultra-fast capillary pressure and resistivity index.



Eichmann et al.

PAGES 438–447

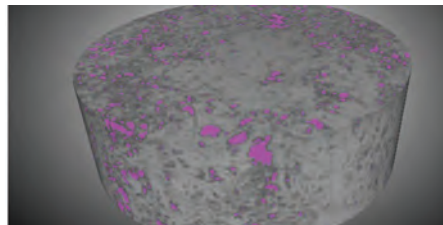
This paper demonstrates a new workflow that leverages terahertz time-domain spectroscopy (THz-TDS) imaging to quickly map lateral variations in microporosity using the THz attenuation due to water-filled pores. By imparting preselected saturation states, tracking sample mass, and obtaining THz-TDS maps, the method measures the amount of microporosity while providing a map of the microporosity distribution in carbonate rocks.



Fernandes et al.

PAGES 325–339

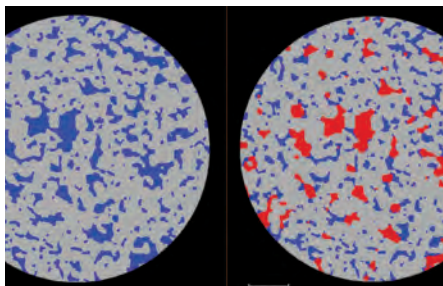
When obtaining representative conditions of the reservoir regarding initial water saturation (S_{wi}), fluids distribution and saturation profile homogeneity are important parameters when initializing rock samples by the restored state method. Nonetheless, the classic techniques for setting S_{wi} present clear limitations in terms of profile homogeneity, experimental duration, and control of the target value of S_{wi} . Therefore, we propose a new Hybrid Drainage Technique that combines the advantages of the viscous oilflood and porous plate methods for performing primary drainage in significantly reduced experimental time, setting a uniform saturation profile at a targeted S_{wi} .



Funk et al.

PAGES 421–437

By viewing nuclear magnetic resonance and dielectric relaxation time distributions as comparable probes of molecular motion in porous media, a technique to map dielectric dispersion onto standard NMR T_2 distributions has been developed. The mapping approach is validated with micro-CT imaging and conventional petrophysical models for formation factor and NMR diffusion in conventional carbonate samples.

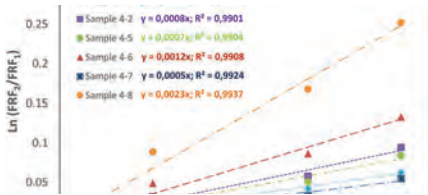


Gao et al.

PAGES 368–383

To describe and measure the trapped gas saturation (S_{gr}) accurately, high-resolution X-ray computed tomography (micro-CT) imaging techniques are used to directly visualize the pore-scale processes during gas trapping. Our experimental insights show that due to ripening effects in the pore space, even for (outside of the rock) pre-equilibrated brine, the remaining gas saturation continually decreased with more (pre-equilibrated) brine injected and even after the brine injection was stopped, resulting in very low remaining gas saturation values at the pore-scale level.

JUNE 2023 PAPER SUMMARIES



Nourani et al.

PAGES 353–366

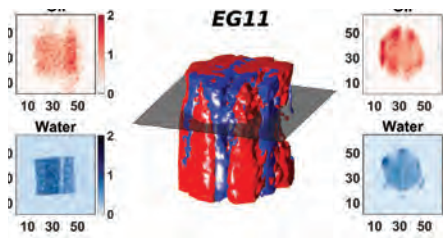
In order to predict the formation resistivity factor (*FRF*) and resistivity index (*RI*) under overburden pressure conditions, analytical models were developed based on rock resistivity modulus (*RRM*), true resistivity modulus (*TRM*), and Archie's equation. A variety of core data from sandstone and carbonate reservoirs has been used to validate the proposed *FRF* models.



Olszowska et al.

PAGES 402–419

A new laboratory method is presented for characterizing short-range variations in elastic properties of reservoir rocks. This method involves ultrasonic angle-dependent measurements of reflected waves, allowing estimation of P- and S-wave velocity as well as density. The obtained measurements provide continuous descriptions of sample complexity.



Zamiri et al.

PAGES 384–401

Application of magnetic resonance measurements for shale characterization has become increasingly common in the petroleum industry. However, the short magnetic resonance lifetimes of shale rocks prevent quantitative signal detection. In this work, FID-based methods were used to quantify water, oil, and kerogen in the shale samples and provide separate images of oil and water on the centimeter scale.